

HIGGS

Hydrogen in Gas Grids

A systematic validation approach at various admixture levels into high-pressure grids

D4.3

Update on test results

Date 28th February 2023 (M38)
Grant Number 875091
Author(s) **Virginia Madina**¹, Jorge Aragón,¹ Ekain Fernández,¹ Vanesa Gil^{2,3}, Javier Sánchez², Alberto Cerezo⁴,
1 Tecnalia
2 Fundación Hidrógeno Aragón
3 ARAID
4 Redexis
Author printed in bold is the contact person

Status Started / Draft / Consolidated / Review / Approved / **Submitted** / Accepted by the EC / Rework [use bold style for current state]

Dissemination level:

PU **Public**

RE Restricted to a group specified by the consortium*

PP Restricted to other programme participants*

CO Confidential, only for members of the consortium*

*(including the Commission Services)



This project has received funding from the Fuel Cells and Hydrogen 2 Joint Undertaking (now Clean Hydrogen Partnership) under Grant Agreement No. 875091 'HIGGS'. This Joint Undertaking receives support from the European Union's Horizon 2020 Research and Innovation program, Hydrogen Europe and Hydrogen Europe Research.

Document history

Version	Date	Description
1.1	2023-05-11	First draft
1.2	2023-05-12	First revision of draft by all partners
1.3	2023-05-16	Consolidated final version

The contents of this document are provided “AS IS”. It reflects only the authors’ view and the JU is not responsible for any use that may be made of the information it contains.

Pending for approval

Table of Contents

Document history	2
Acronyms	6
Executive Summary	7
1 Objective	9
2 Introduction	10
3 Test methods for the testing platform at FHA	11
4 Results from the 2nd and 3rd experimental campaigns	15
4.1 Inspection of equipment from the dynamic section for hydrogen damage evaluation (2 nd campaign)	15
4.2 Inspection of valves from the static section for hydrogen damage evaluation (2 nd campaign)	17
4.2.1 Ball valve analysis (2 nd campaign).....	17
4.3 API 5L steel specimens constant displacement tests (2 nd and 3 rd campaigns).....	19
4.3.1 C-ring specimens	20
4.3.2 4pb specimens.....	21
4.3.3 CT-WOL specimens.....	23
4.4 Gas tightness tests (3 rd campaign. Tentative results)	25
5 Slow Strain Rate Tests	28
6 Conclusions	29
Bibliography and References	30
Acknowledgements	31

List of Figures

Figure 1. Picture of HIGGS experimental platform	11
Figure 2. Parts of the pressure regulator (left) and detail of some of the pilot O-rings inspected (right)	15
Figure 3: Detail of the gasket from the pressure regulator	15
Figure 4. Pilot guide ring from the pressure regulator.....	16
Figure 5. Pre-pilot pressure regulator components (left) and detail of filter cartridge (right).....	16
Figure 6. Pre-pilot membrane (left) and pad (right).....	16
Figure 7. Spirometallic gaskets	16
Figure 8. Components of the ALFA VALVOLE ball valve (n° 4) (left) showing detail of the graphoil (centre) and Teflon seals (right)	17
Figure 9. Components of the KURVALF plug valve (left) showing detail of the O-rings (middle) and the graphoil and Teflon seals (right)	17
Figure 10. Photograph showing detail of the ball valve sent to TECNALIA (right) and data sheet supplied by the manufacturer (left)	18
Figure 11. Photographs showing details of the ball valve	18
Figure 12. Photographs showing detail of the deformed TFM seat.....	19
Figure 13. Photograph showing detail of the ball (left) and SEM micrograph of abraded area (centre) with EDS spectrum of this zone (right)	19
Figure 14. EDS spectrum of corrosion products in valve closure zone.....	19
Figure 15. Test specimens inside the pig trap in the loop experimental platform at FHA at the beginning of the 2 nd experimental campaign (M30) (left) and once concluded (M33) (right)	20
Figure 16. Detail of tested C-ring specimens (3 rd campaign)	20
Figure 17. Resin embedded notched C-ring cross sections (up) and optical micrographs from steel grades X60 (down-left) and X42 (down-right) (2 nd campaign).....	21
Figure 18. Tested X70 base and welded 4pb specimens supported in the loading jig (3 rd campaign)	22
Figure 19. Optical micrographs of metallographic sections of X52 (left) and X70 (right) welded steel specimens (2 nd campaign)	22
Figure 20. Resin embedded cross sections of 4pb X52 and X70 welded steel specimens (left) and optical micrograph of metallographic section of X70 welded joint (right) (3 rd campaign)	22
Figure 21. Rack with tested CT bolt loaded specimens in the 2 nd campaign (left) and in the 3 rd campaign (right).....	23
Figure 22. Heat tinted fracture surface of CT-WOL X60 specimen (up) and SEM micrographs of the fatigue pre-crack surface (down-left) and detail of the crack advancing front (down-right).....	24
Figure 23. Heat tinted fracture surface of tested CT-WOL X70 specimen (up) and SEM micrographs of the fracture surface in the fatigue pre-crack and in the crack front (down)	24
Figure 24. Evolution of the pressure (top left), the P/Z-T quotient (top right) and gas composition in %mol H ₂ (down) in each line of the static section during the second experimental campaign.....	26
Figure 25. Picture of part of the static section of the testing platform. Red arrows show the point where hydrogen leakages were detected.....	27

List of Tables

Table 1. Guide for finding results of the different experimental campaigns in HIGGS' deliverables .	8
---	---

D4.3 Update on test results

Table 2. List of valves tested in the static section of the R&D facility.....	11
Table 3. Testing elements in the dynamic section of the testing platform	12
Table 4. Properties of API5L steel pipes under study	13
Table 5. Types of constant displacement specimens used in the testing platform	13
Table 6. Test conditions for the four experimental campaigns.....	20
Table 7. Summary of test results for the C-ring tests.....	21
Table 8. Summary of test results for the 4pb tests	23
Table 9: Summary of test results for the CT-WOL tests	25

Pending for approval

Acronyms

API	American Petroleum Institute
CT	Compact Tension
EDS	Energy Dispersive X-Ray Spectroscopy
FHA	Fundación Hidrógeno Aragón
GTAW	Gas Tungsten Arc Welding
HAZ	Heat Affected Zone
ISO	International Organization for Standardization
NG	Natural Gas
SEM	Scanning Electron Microscope
SSRT	Slow Strain Rate Test
TFM	Modified Teflon
WOL	Wedge Opening Load
4pb	Four-point bend (specimen)

Pending for approval

Executive Summary

Deliverable D4.3 gathers the results obtained in the different tests performed during the 2nd and 3rd experimental campaigns, carried out in the R&D testing platform built in WP3 at Fundación Hidrógeno Aragón (FHA). This R&D facility aims to reproduce a natural gas transmission grid at smaller scale, where different testing components, materials and equipment are exposed to hydrogen. Four different kind of tests have been performed in the platform during these two experimental campaigns:

- Gas tightness tests of representative valves of the natural gas (NG) grid to identify possible leakages when operated with hydrogen. D4.2 already collected the results of the gas tightness tests of the valves from the 1st and 2nd campaigns. D5.3 shows preliminary tests of the third campaign.
- Constant displacement tests carried out on API 5L steel specimens grades X42, X52, X60 and X70, for hydrogen embrittlement evaluation of representative carbon steels in the NG grid. D4.3 collects the results from the 2nd and 3rd experimental campaign
- Inspection of equipment (pilot-operated pressure regulator and cartridge filter) components from the dynamic section after the 2nd campaign, for hydrogen damage evaluation.
- Inspection of components of the valves in the static section for hydrogen damage evaluation. D4.3 collects the results obtained in the inspection of the valves after the 2nd campaign, together with the characterization of the screwed ball valve which presented a gas leakage after the emptying and inertization process at the end of the 2nd campaign. These valves are the same used as testing items in the gas tightness tests described above.

The 2nd experimental campaign consisted in the 20/76 (%/mol) H₂/CH₄ blend gas condition, with H₂S up to 11 ppmv and CO₂ (4 mol%) as impurities. These amounts correspond to the maximum concentration of these impurities in NG according to the current regulation in Germany and Spain. The gas mixture for the 3rd campaign was made up of 30/66 (mol %/%) H₂/CH₄ with the same concentration of impurities than those contemplated for the 2nd campaign. Test pressure for both experimental campaigns was 80 bar, with a duration of 2300 hours for the 2nd campaign and 2100 hours for the 3rd campaign.

No cracks or other kind of damage were found on the valves and parts of the equipment exposed to the 20/76 (mol%/%) H₂/CH₄ blend. The C-ring, 4pb and CT-WOL specimens machined from the API5L steel pipes grades X42 to X70 did not show cracking or precrack growth after testing in the 20/76 and 30/66 (mol%/%) H₂/CH₄ blends with H₂S and CO₂ impurities. Therefore, in the tests to evaluate the compatibility of the steels using constant deformation specimens no signs of embrittlement are observed for the 2nd and 3rd experimental campaigns.

The results of the 3rd campaign are still preliminary, but a critical gas loss could be already detected for screwed ball valves, which may make them not suitable for hydrogen service with 30 mol% blends. The possibility of gas stratification must be monitored during the final period of the test.

D4.3 Update on test results

Table 1 shows a list of the different tests performed in each campaign in the testing platform and the deliverable number in which they can be found.

Table 1. Guide for finding results of the different experimental campaigns in HIGGS' deliverables

Campaign	Test	Report containing the results
1st 20 mol% H ₂ blend	Gas tightness tests	D4.2
	Constant displacement tests carried out on API 5L steel specimens	D4.2
	Inspection of equipment	D4.2
	Inspection of valves	D4.2
	Gas separation with membrane prototype	D4.2
2 nd 20 mol% H ₂ blend+H ₂ S+CO ₂	Gas tightness tests	D4.2
	Constant displacement tests carried out on API 5L steel specimens	D4.3
	Inspection of equipment	D4.3
	Inspection of valves	D4.3
3 30 mol% H ₂ blend+H ₂ S+CO ₂	Gas tightness tests	Preliminary results in D4.3. Final results in D4.4
	Constant displacement tests carried out on API 5L steel specimens	D4.3
	Inspection of equipment	Ongoing. To be shown in D4.4
	Inspection of valves	Ongoing. To be shown in D4.4
4 100 %mol H ₂	Gas tightness tests	Not started yet. To be shown in D4.4
	Constant displacement tests carried out on API 5L steel specimens	Not started yet. To be shown in D4.4
	Inspection of equipment	Not started yet. To be shown in D4.4
	Inspection of valves	Not started yet. To be shown in D4.4

1 Objective

The main objective of this deliverable is to show the results obtained in some of the tests carried out during the 2nd and 3rd experimental campaigns, at the R&D testing platform at FHA.

The following results are included in this document:

- Results from the inspection of valves and equipment tested during the 2nd campaign.
- Results from the analysis of the constant displacement tests carried out for the API 5L steels during the 2nd and 3rd campaigns.
- Tentative results on gas tightness test of the 3rd campaign.

Pending for approval

2 Introduction

Blending hydrogen with NG may have an impact on safety issues, pipeline integrity, and gas quality. The potential leakage rate of hydrogen is much larger than that of NG through the same sized leak. Besides, possible hydrogen embrittlement mechanism may occur under the transport pressures and the combustion properties change when hydrogen is added to NG, with direct impact on end users.

Research to assess the impact of hydrogen on the NG infrastructure is therefore necessary when analysing its suitability for hydrogen transport, with special focus on hydrogen embrittlement and gas leakage. Gas separation technologies are also necessary to obtain high-concentrated methane steams from admixture flows below 20 mol% H₂.

Hydrogen embrittlement is a process in which the tensile ductility of a material working on hydrogen environment is significantly reduced because of the introduction of hydrogen atoms in its lattice. Additionally, the fracture toughness and fatigue strength of this material decreases. The severity of these manifestations of hydrogen embrittlement depends on mechanical, environmental and material (microstructure and tensile strength, principally) variables. It is critical to ensure the resistance of pipelines materials and other metallic materials in the grid to this phenomenon, for a safe and efficient hydrogen transport.

The testing platform built at FHA is an R&D setup that tries to replicate a NG transmission facility in which real pipes, components and equipment of high-pressure grids have been installed to expose them to hydrogen blends at 80 bar pressure, to assess the suitability of high-pressure NG grids for the transport of H₂/NG blends or even 100% H₂ gas. For this purpose, gas tightness tests, constant strain mechanical tests and gas permeation tests are carried out in the HIGGS project.

The four experimental campaigns have considered different gas compositions:

- 1st campaign: 20/80 mol (%/%) H₂/CH₄ blend, from M22 to M26
- 2nd campaign: 20/76 mol (%/%)H₂/CH₄ + H₂S +CO₂ blend, from M30 to M33
- 3rd campaign: 30/66 mol(%/%)H₂/CH₄ + H₂S +CO₂ blend, from M36 to M39 (still ongoing in the static section due to a delay reassembling the test valves)
- 4th campaign: 100 mol%H₂, from M41 to M44

Test pressure for all the experimental campaigns is 80 bar.

3 Test methods for the testing platform at FHA

As reported in D3.1 and D3.3, the testing platform consists in a static section, a dynamic section, and a membrane prototype. A picture of this facility can be seen in Figure 1.



Figure 1. Picture of HIGGS experimental platform

The different tests carried out in the different sections of the platform were explained in deliverable D4.2. As a reminder five different kind of tests have been performed:

- **Gas tightness tests** of representative valves of the NG grid to identify possible leakages when operated with hydrogen. Specific information about the testing valves can be seen in Table 2.

Table 2. List of valves tested in the static section of the R&D facility

Element	Manufacturer	Model	Additional	com- ments
Ball Valve	ALFA VALVOLE	ALFA-606/FB Body	Split	ANSI 600# Lever
Lug-type butterfly Valve	DIDTEK	LUG – LEAKAGE CLASS	ZERO	ANSI 600# Gear- box & handwheel
Plug valve	KURVALF	RF-VP		ANSI 600# Lever

D4.3 Update on test results

Needle valve	ALFA VALVOLE	A20T 800LB	ANSI 600#
Ball valve	NUOVAFIMA	BSV/VV	ANSI 600#

- **Hydrogen damage inspection** of these same valves. At the end of the gas tightness tests, the flanged valves are disassembled, and their different parts inspected to detect the presence of cracks or any other damage, that could be attributed to hydrogen exposure.
- **Hydrogen damage inspection** of the equipment located in the dynamic section of the testing platform. As testing equipment, a filter, a pressure regulator, and a gas meter have been installed, building a kind of Metering and Regulation Station of the transmission grid. The characteristic of this equipment is given in Table 3.

Table 3. Testing elements in the dynamic section of the testing platform

Element	Manufacturer	Model	Connection and technical standard	Additional comments
Cartridge Filter	FIORENTINI	HFA/1	RF-1"	ANSI 600#
Pilot-operated pressure regulator	FIORENTINI	REFLUX-819 P.207/A+R14 SB-105	RF-1"	ANSI 600#
Turbine flowmeter	ELSTER	TRZ2 G100 A1R/A 1S	RF-3"	ANSI 600#
Pressure indicator	NUOVAFIMA	MGS18/2/A	thread 1/2" NPT- M	DN 100 KL0,6% 0-100 bar
Pressure Transmitter	YOKOGAWA	EJA530E- JCS7N-014EN /KU22	thread 1/2" NPT- M	0-100 bar 4-20 mA Display
Temperature transmitter	YOKOGAWA	YTA610	-	PT100 Sensor -50 +200 °C Display

- **Constant displacement tests** carried out on API 5L steel specimens grades X42, X52, X60 and X70, for hydrogen embrittlement evaluation. The as received chemical composition,

D4.3 Update on test results

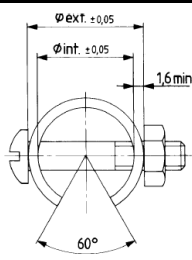
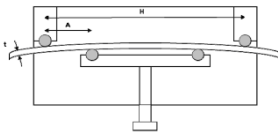
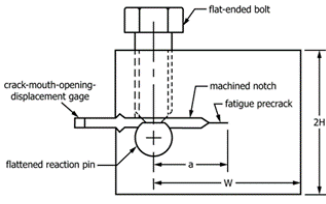
mechanical properties and metal microstructure of the base and welded steels was collected in deliverables D3.1 and D4.1. Table 4; **Error! No se encuentra el origen de la referencia.** summarizes important aspects of the four steels under study. Details of the normalized C-ring, four-point bend (4pb) and CT-WOL (Compact Tension Wedge Opening Load) constant displacement specimens, were given in deliverable D4.2. Details of the three normalized constant displacement specimens are summarized in Table 5.

Table 4. Properties of API5L steel pipes under study

API 5L steel grade	Nominal diameter (in)	Outside diameter (mm/in)	Wall thickness (mm) ¹	Yield strength (MPa)		Ultimate tensile strength (MPa)		Welding procedure / filler material	Microstructure (base steel)
				Tensile testing (ISO 6892) ² [1]	API 5L (min.)	Tensile testing (ISO 6892)	API 5L (min.)		
X42	6	168.3/6.625	6.9	451	290	542	415	GTAW ³ ER70S-6	Ferrite + pearlite
X52	6	168.3/6.625	7.8	440	360	514	460	GTAW / ER70S-6	Ferrite + pearlite
X60	6	168.3/6.625	7.8	510	415	581	520	GTAW / ER90S-B3	Bainite
X70	16	406.4/16.0	8.2	549	485	675	570	GTAW / ER90S-B3	Ferrite + bainite

¹thickness obtained from metallographic cross sections
²average values of two tensile tests
³Gas Tungsten Arc Welding (GTAW)

Table 5. Types of constant displacement specimens used in the testing platform

Type of specimen	Constant displacement specimens		
	C-ring	4pb	CT-WOL
Geometry			
Condition	Smooth and notched base specimens	Smooth base and welded specimens	Notched pre-cracked base and welded specimens
Applicable standards	ISO 7539-5, ASTM G38	ISO 7539-2, ASTM G39	ISO 7539-6, ASTM E1681, ASTM E399

D4.3 Update on test results

Steel grades	X42, X52, X60	X52, X70	X52, X60, X70
Environment	From 20 mol% H ₂ in CH ₄ to 100 mol% H ₂ - 80 bar /ambient temperature		
Test duration	2300-3000 hours		
Post testing evaluation	<ul style="list-style-type: none"> - Evidence of cracking in C-ring and 4-pb specimens - Crack growth in CT-WOL specimens - Metallographic/fractographic examination by optical and SEM microscopy 		

- **H₂/CH₄ gas separation tests** with a membrane prototype. A detailed description of the two Pd-based membrane prototypes and the gas separation performance of each of them was given in D4.2. The gas separation tests have been only carried out in the first experimental campaign, since this campaign does not incorporate impurities that could damage the membrane.

Pending for approval

4 Results from the 2nd and 3rd experimental campaigns

4.1 Inspection of equipment from the dynamic section for hydrogen damage evaluation (2nd campaign)

The pilot-operated pressure regulator and cartridge filter tested in the dynamic section of the testing platform, were disassembled at the end of the test and their different parts examined with the aid of a stereo microscope with a camera, to detect cracking or other type of hydrogen damage such as blistering. Apart to linear or scratch abrasion in certain components, mainly generated in the process of disassembling, no clear signs of hydrogen damage were observed on the different parts inspected. Figure 2 to Figure 7 show the general appearance and some more detailed analysis of some of the examined items. No blistering was observed in the plastic or polymeric components at the time of removal from the testing platform. No cracking was detected for any of the metal components.



Figure 2. Parts of the pressure regulator (left) and detail of some of the pilot O-rings inspected (right)

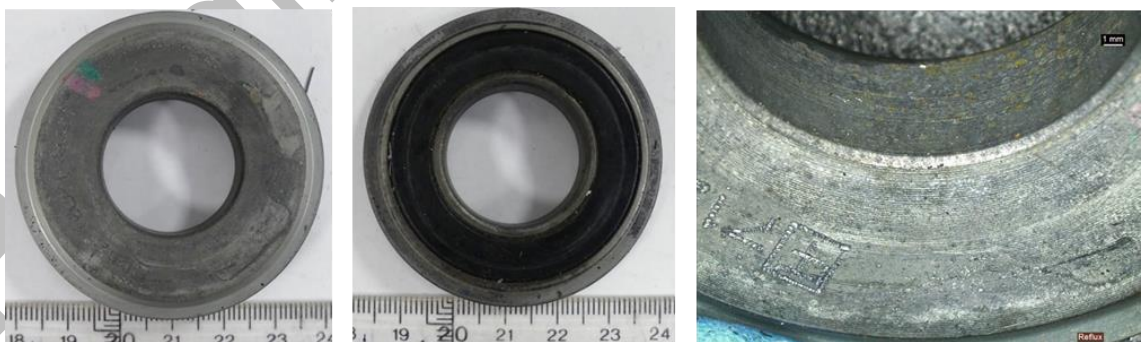


Figure 3: Detail of the gasket from the pressure regulator



Figure 4. Pilot guide ring from the pressure regulator



Figure 5. Pre-pilot pressure regulator components (left) and detail of filter cartridge (right)

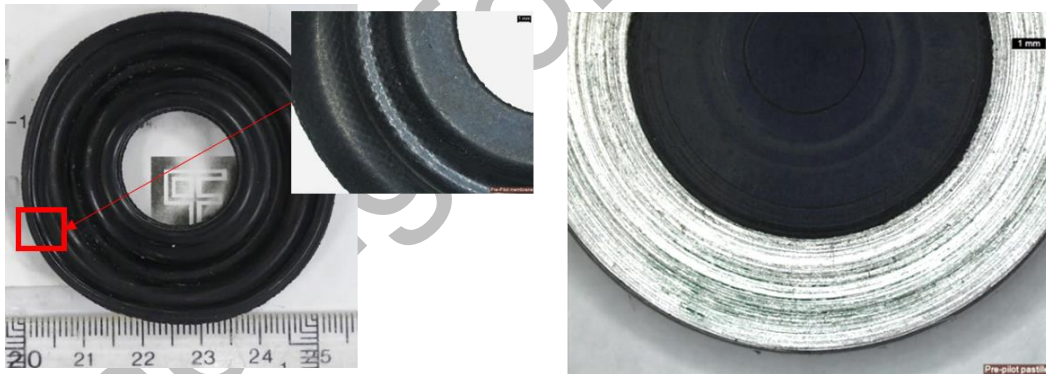


Figure 6. Pre-pilot membrane (left) and pad (right)

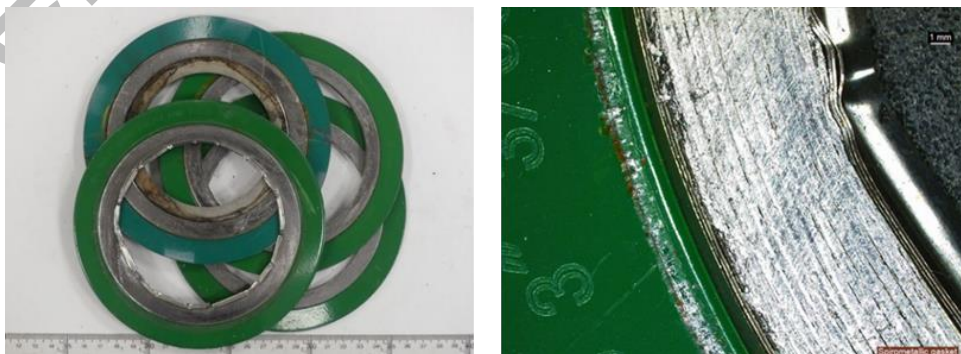


Figure 7. Spirometallic gaskets

4.2 Inspection of valves from the static section for hydrogen damage evaluation (2nd campaign)

The main body of the plug, the ball and the butterfly valves installed in the static section of the R&D platform (see Table 1), were disassembled at the end of the 2nd experimental campaign and inspected to detect signs of hydrogen damage. In general, the Teflon seals did not show any significant damage, except for that which may have been generated in the process of disassembling of the valve. The seal bodies made of Graphoil were in many cases broken or fragmented, most probably due to the process of dismantling of the valve, as it is a very soft and flexible material. Figure 8 and Figure 9 show the general appearance of some of the examined items.



Figure 8. Components of the ALFA VALVOLE ball valve (n° 4) (left) showing detail of the graphoil (centre) and Teflon seals (right)



Figure 9. Components of the KURVALF plug valve (left) showing detail of the O-rings (middle) and the graphoil and Teflon seals (right)

4.2.1 Ball valve analysis (2nd campaign)

As already reported in D4.2, a gas leakage was detected in one of the testing ball valves at the end of the 2nd campaign. This failure occurred after emptying the platform and filling it again at 4 bar with nitrogen. The valve was sent to Tecnia to evaluate the type of damage observed in the valve.

Figure 10 and Figure 11 show details of this screwed ball valve. The visual inspection of the valve prior to its disassembly revealed a quite significant corrosion in the thread exposed to the air (atmosphere), while the thread in contact to the H₂/CH₄ blend was not corroded, which is logical since the H₂/CH₄ gas mixture is not corrosive.

D4.3 Update on test results

The valve was cut to unscrew the body and closure (probably blocked due to corrosion). A marked not uniform deformation was observed in the Teflon seat located near the closure (see Figure 12), being this fact the most likely cause of the leakage observed in the ball valve. It seems that the ball could not be fully aligned with the seat, so the seat was pushed when the valve was closed and deformed by the ball when opened.

A very little abrasive effect was observed in the stainless-steel ball, mainly attributed to the generation of corrosion products from the carbon steel zinc coated body/closure (see Figure 13). Corrosion products inside the body of the valve were chemically characterized by energy dispersive x-ray spectroscopy (EDS), using a microanalyzer coupled to the SEM (scanning electron microscope). EDS spectra indicated that corrosion products were mainly constituted of zinc (Zn), iron (Fe) and oxygen (O) as zinc and iron oxides (see Figure 14).

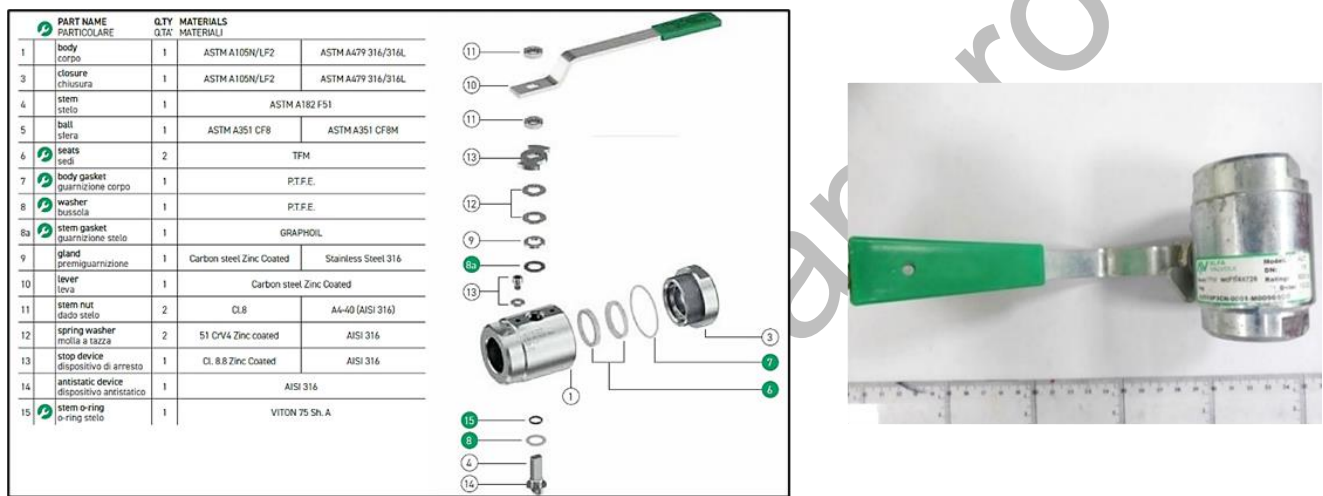


Figure 10. Photograph showing detail of the ball valve sent to TECNALIA (right) and data sheet supplied by the manufacturer (left)

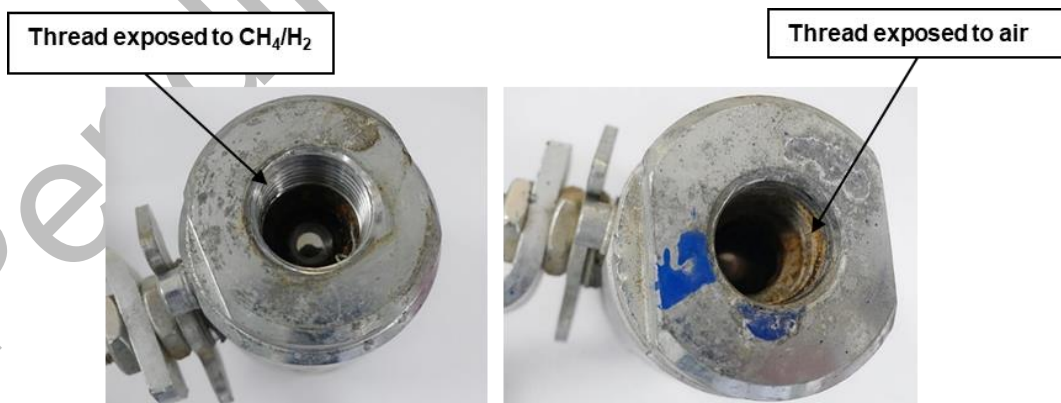


Figure 11. Photographs showing details of the ball valve

D4.3 Update on test results



Figure 12. Photographs showing detail of the deformed TFM seat

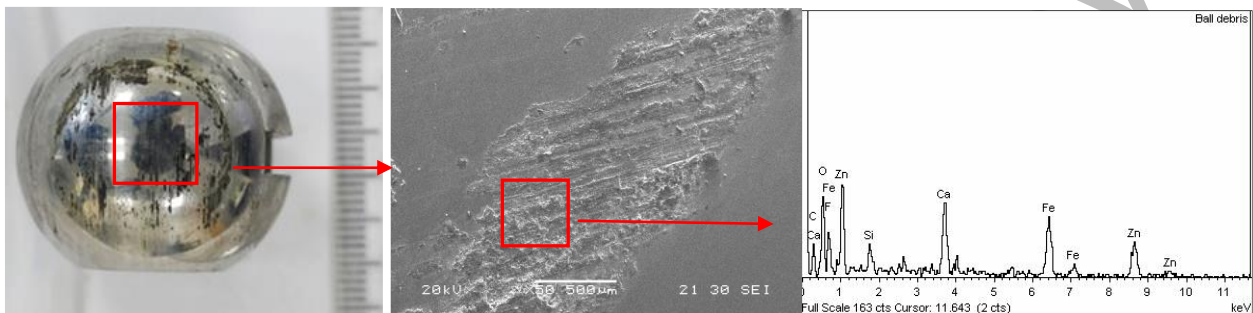


Figure 13. Photograph showing detail of the ball (left) and SEM micrograph of abraded area (centre) with EDS spectrum of this zone (right)

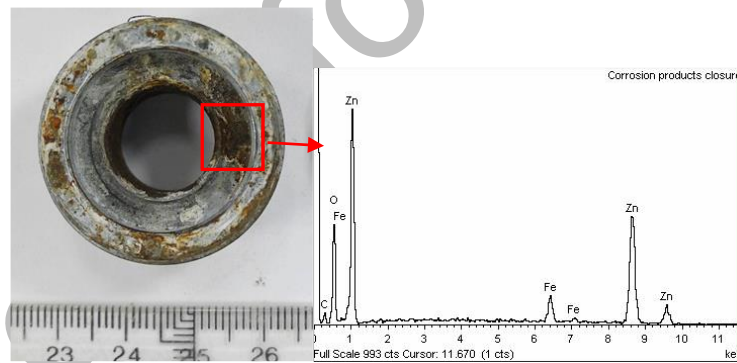


Figure 14. EDS spectrum of corrosion products in valve closure zone

4.3 API 5L steel specimens constant displacement tests (2nd and 3rd campaigns)

The constant displacement steel specimens were located inside the pig trap in the loop experimental platform at FHA and exposed to the gas atmospheres. At the conclusion of the test, the dynamic section of the loop was depressurized and purged with nitrogen and the pig trap was open. Figure 15 shows the aspect of the racks with the steel specimens inside the pig trap. Experimental conditions for the experimental campaigns are summarized in Table 6.

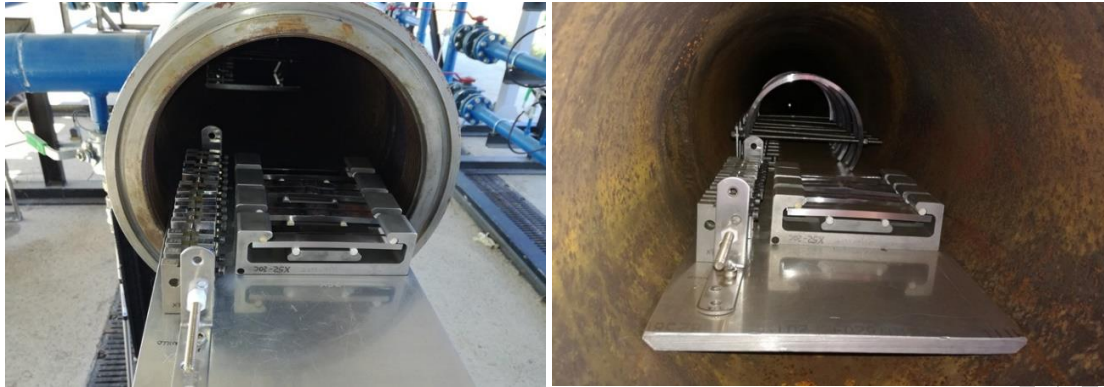


Figure 15. Test specimens inside the pig trap in the loop experimental platform at FHA at the beginning of the 2nd experimental campaign (M30) (left) and once concluded (M33) (right)

Table 6. Test conditions for the four experimental campaigns

Campaign number	Gas composition	Pressure (bar)	Duration (hours)
1	20%H ₂ / 80%CH ₄	80 bar	3000
2	20%H ₂ / 76%CH ₄ + 11ppmv H ₂ S+ CO ₂ (4 mol%)		2300
3	30%H ₂ / 66%CH ₄ + 11ppmv H ₂ S+ CO ₂ (4 mol%)		2100
4	100% H ₂		-

The results obtained in the constant displacement tests carried out in the 2nd and 3rd experimental campaigns are detailed below.

4.3.1 C-ring specimens

Figure 16 shows the appearance of the tested C-ring specimens after the 3rd experimental campaign. No cracks were detected after optical inspection with a LEICA S9i stereo microscope. Metallographic sectioning confirmed the absence of cracks both in base and C-ring notch samples tested in the 2nd and 3rd campaign, as shown in the optical micrographs in Figure 17, corresponding to specimens tested in the 2nd campaign. Table 7 summarizes the results obtained for the C-ring specimens in the three experimental campaigns carried out until now in the experimental platform.

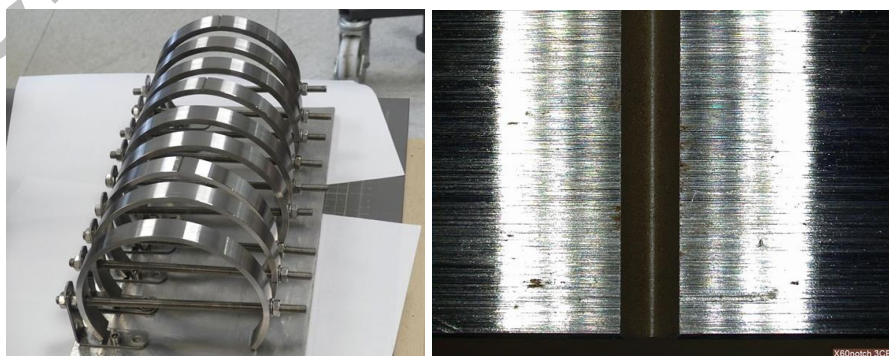


Figure 16. Detail of tested C-ring specimens (3rd campaign)

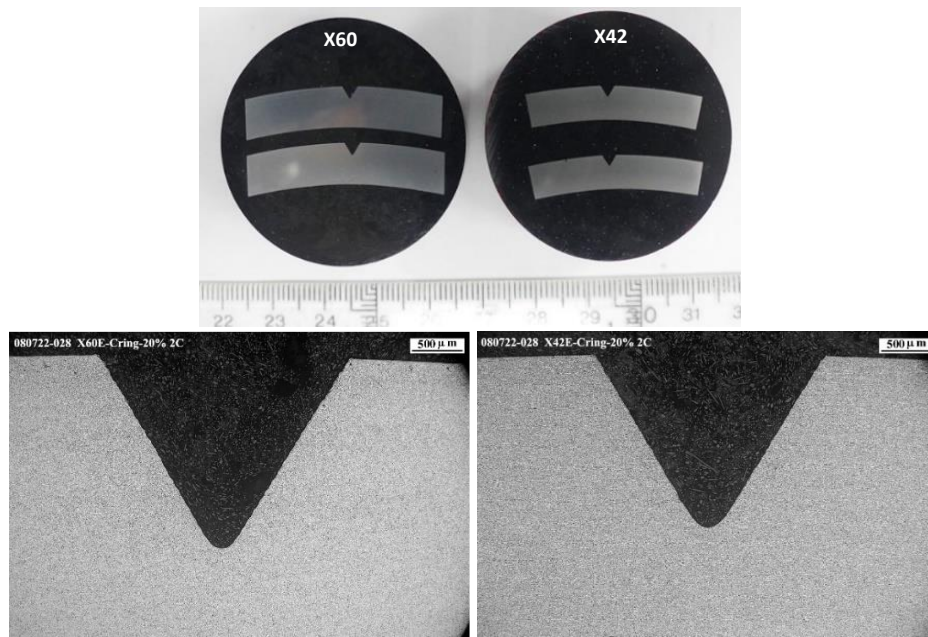


Figure 17. Resin embedded notched C-ring cross sections (up) and optical micrographs from steel grades X60 (down-left) and X42 (down-right) (2nd campaign)

Table 7. Summary of test results for the C-ring tests

Campaign number	Steel grade	Condition	Results
1	X42 base	Smooth /notched	No cracks
	X52 base	Smooth /notched	
	X60 base	Smooth /notched	
2	X42 base	Smooth /notched	No cracks
	X52 base	Smooth /notched	
	X60 base	Smooth /notched	
3	X42 base	Smooth /notched	No cracks
	X52 base	Smooth /notched	
	X60 base	Smooth /notched	

4.3.2 4pb specimens

Figure 18 shows the appearance of welded X70 steel 4pb specimens supported in the loading jig, tested during the 3rd experimental campaign. No cracks were detected during the inspection with a stereo microscope. Metallographic sectioning confirmed the absence of cracks in the base, heat affected zone (HAZ) and weld metal areas both for the specimens tested in the 2nd campaign and for those tested in the 3rd campaign, Figure 20 and Figure 21. Table 8 summarizes the results obtained for the 4pb specimens in the three experimental campaigns carried out till now.

D4.3 Update on test results

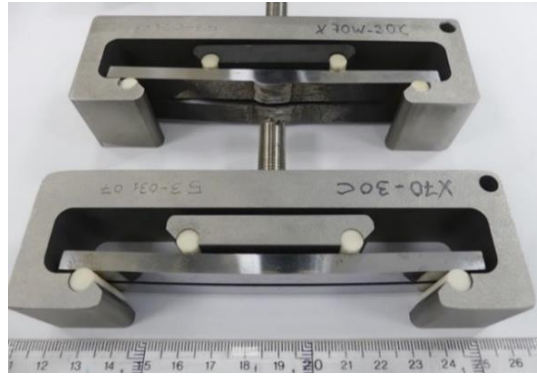


Figure 18. Tested X70 base and welded 4pb specimens supported in the loading jig (3rd campaign)

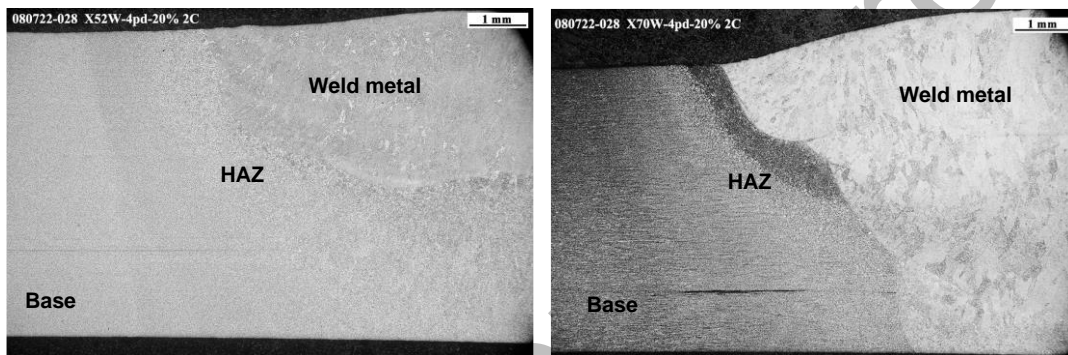


Figure 19. Optical micrographs of metallographic sections of X52 (left) and X70 (right) welded steel specimens (2nd campaign)

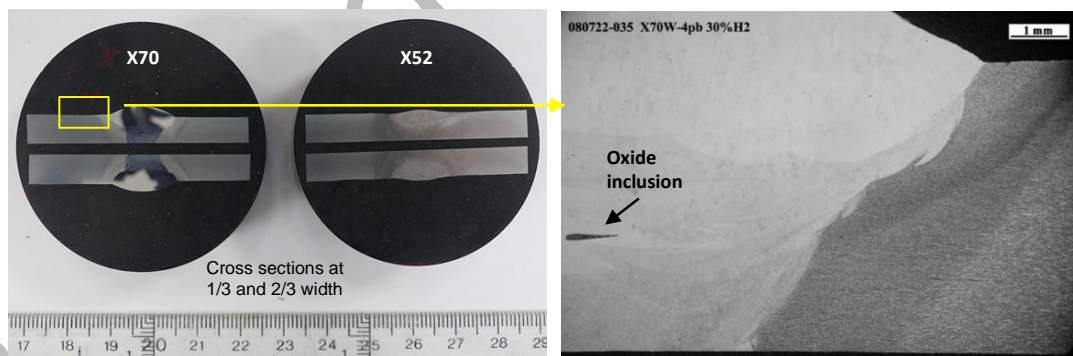


Figure 20. Resin embedded cross sections of 4pb X52 and X70 welded steel specimens (left) and optical micrograph of metallographic section of X70 welded joint (right) (3rd campaign)

Table 8. Summary of test results for the 4pb tests

Campaign number	Steel grade	Results
1	X52 base	No cracks
	X52 welded	
	X70 base	
	X70 welded	
2	X52 base	No cracks
	X52 welded	
	X70 base	
	X70 welded	
3	X52 base	No cracks
	X52 welded	
	X70 base	
	X70 welded	

4.3.3 CT-WOL specimens

Figure 21 shows the appearance of the racks with the CT-WOL specimens tested in the 2nd and 3rd campaigns. The CT specimens were unloaded (removing the bolt) and then heat tinted (30 min at 300 °C) and broken. The fracture surface was examined by SEM to assess if subcritical cracking occurred from the initial fatigue pre-crack. Measurements of the crack front extent were carried out in three positions and the average crack growth in hydrogen was calculated according to ASTM E1681 standard. No hydrogen crack growth was measured for any CT specimen (crack propagation < 0.25 mm). Fracture surface examination revealed the same fracture mode in the fatigue pre-crack and in the crack front (see Figure 222 and Figure 23). The results for these specimens are summarized in Table 9.

As indicated in D4.2, the CT-WOL specimens were machined in accordance with ASTM E1681. In the case of the specimens used in HIGGS, there is an important size limitation due to the small wall thickness of the as received API 5L steel pipes. To be able to use higher K_{IAPP} values, the CT-WOL geometry used in the 3rd campaign has been slightly modified in comparison to that defined in the 1st and 2nd campaign (keeping requirements of standard E1681). This increase in the applied K_{IAPP} value is also shown in Table 9.



Figure 21. Rack with tested CT bolt loaded specimens in the 2nd campaign (left) and in the 3rd campaign (right)

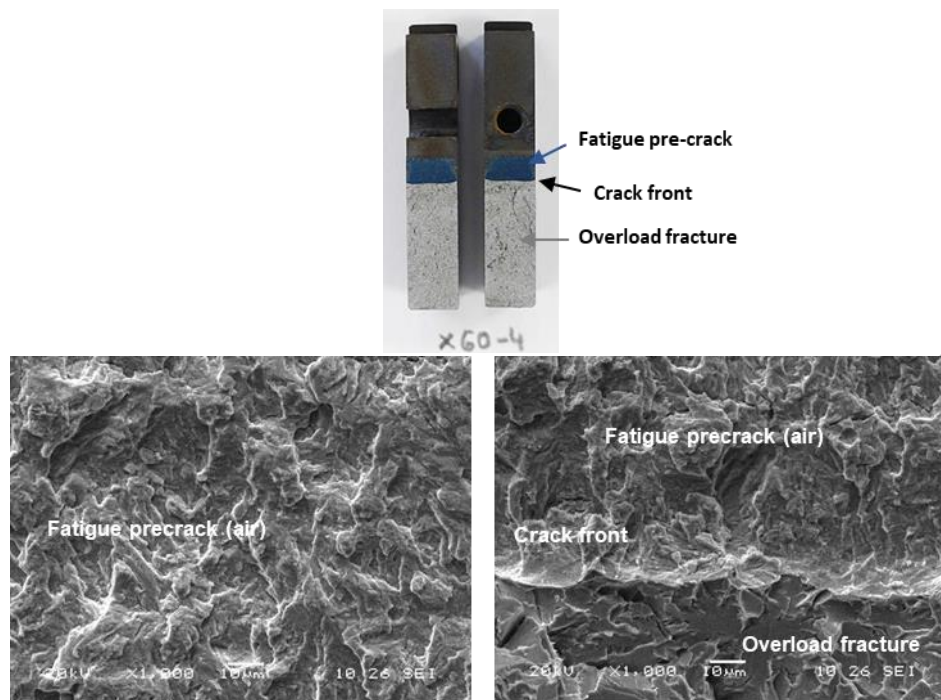


Figure 22. Heat tinted fracture surface of CT-WOL X60 specimen (up) and SEM micrographs of the fatigue pre-crack surface (down-left) and detail of the crack advancing front (down-right)

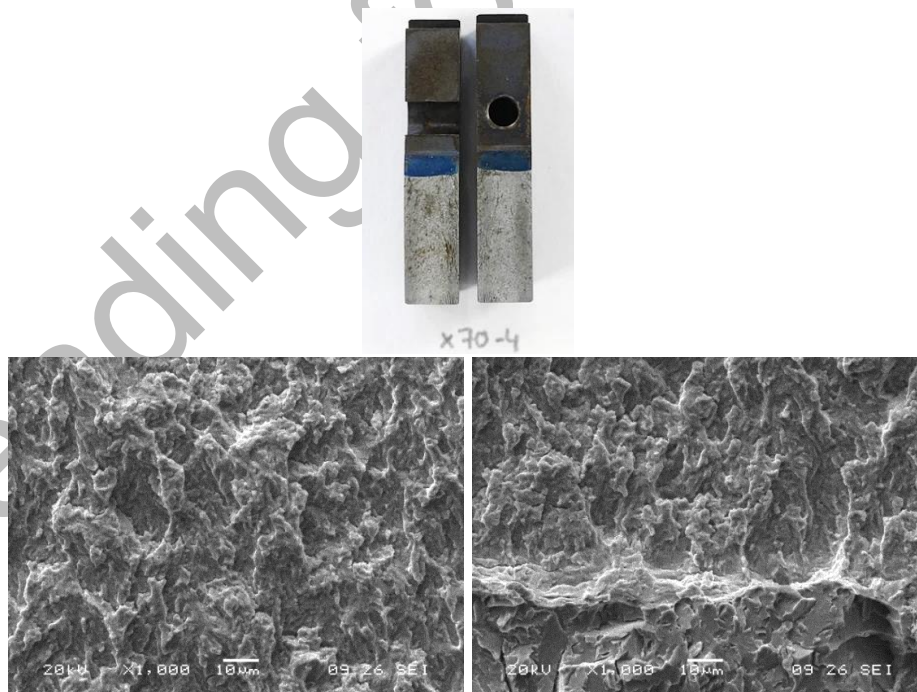


Figure 23. Heat tinted fracture surface of tested CT-WOL X70 specimen (up) and SEM micrographs of the fracture surface in the fatigue pre-crack and in the crack front (down)

Table 9: Summary of test results for the CT-WOL tests

Campaign number	Steel grade	Test duration (hours)	Notch position / crack plane orientation	Applied initial stress intensity (K_{IAPP}) in MPam ^{1/2}	Crack propagation after hydrogen exposure
1	X52	3070	Base / TL	32	<0.25mm
	X52 (HAZ)		Weld / TL	32	<0.25mm
	X70		Base / TL	41	<0.25mm
	X70 (HAZ)		Weld / TL	41	<0.25mm
2	X52	2300	Base / TL	32	<0.25mm
	X52 (weld)		Weld / TL	32	<0.25mm
	X70		Base / TL	41	<0.25mm
	X70 weld		Weld / TL	41	<0.25mm
3	X60	2100	Base / TL	45	<0.25mm
	X70		Base / TL	55	<0.25mm
	X70 weld		Weld / TL	41	<0.25mm

K_{IAPP} =Stress intensity factor applied to the fixed displacement WOL specimen

4.4 Gas tightness tests (3rd campaign. Tentative results)

The tightness of the valves considered in Table 2 is being tested according to the methodology explained in section 3.at 80 bar with the 30 mol% H₂ blend. The test is still ongoing, but the results obtained so far during the first 1400 h are depicted in Figure 24.The evolution of the pressure and the composition of the gas (mol% H₂) for each line of the static section during the time of the experiment is given in Figure 24 (left). P/Z·T versus time is also plotted in Figure 24 (middle) to check the evolution of this relationship during the test This quotient must remain constant in a close system as long as no gas flows out of the system. The compressibility factor has been calculated using the API Soave-Redlich Kwong equation of state for each pressure and temperature value registered by the transmitters in the platform. See D4.2 for more details about the methodology. Finally, Figure 24 (right) shows the hydrogen concentration each line during the test.

D4.3 Update on test results

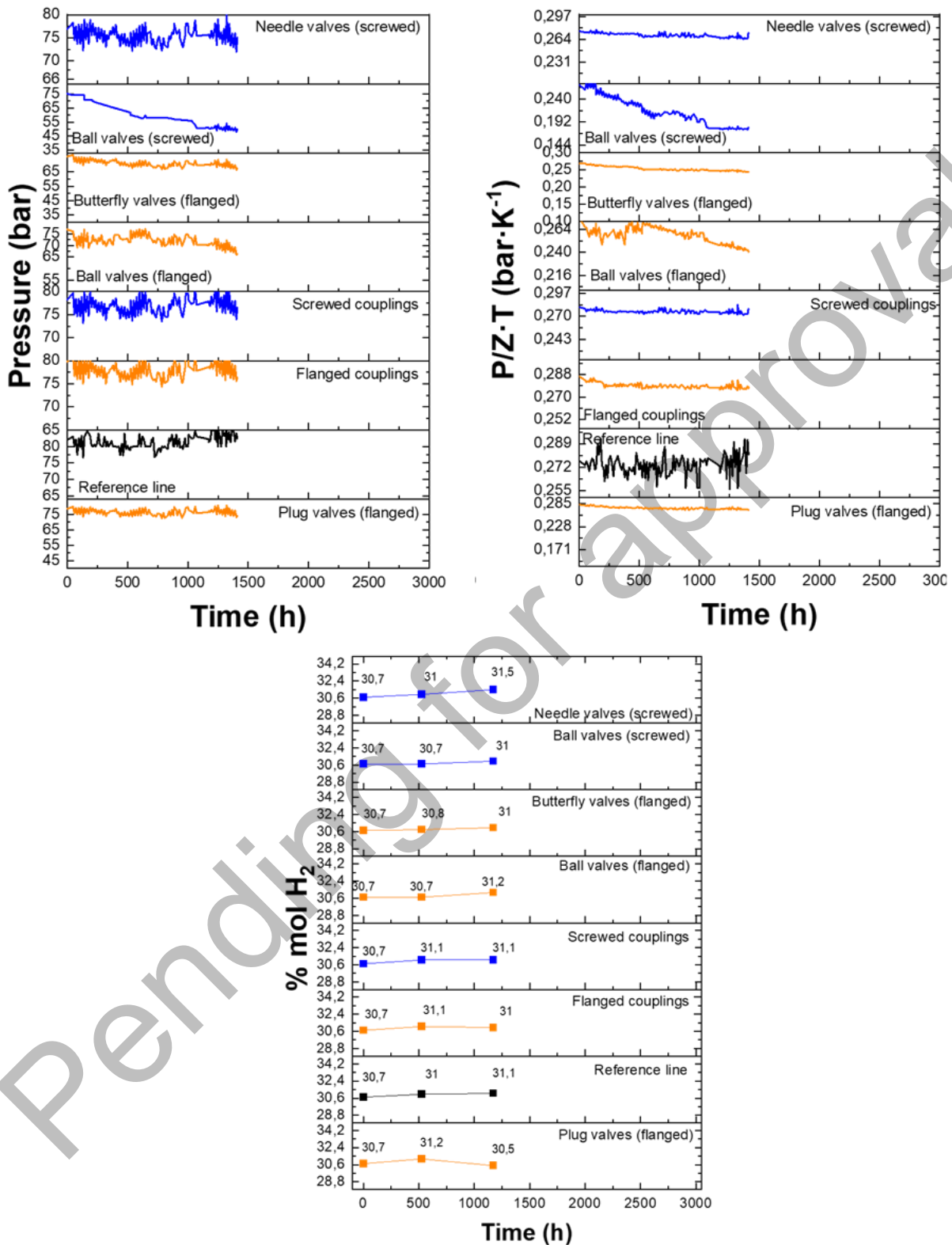


Figure 24. Evolution of the pressure (top left), the P/Z·T quotient (top right) and gas composition in %mol H₂ (down) in each line of the static section during the second experimental campaign

D4.3 Update on test results

So far, most valves and couplings remain tight. There is, however, a critical leakage in the line containing screwed ball valves, where the pressure has dropped almost 30 bar during this first stage of the test. This leakage is due to a lack of internal sealing capacity in this component, since constant hydrogen concentrations up to 1mol% can be detected with a gas detector at the point depicted in Figure 25. This fact occurred for all the three testing valves, so this specific kind of valves may not be suitable for hydrogen service at such levels of blend. Regarding the hydrogen concentration in the lines, it is surprising how the hydrogen level seems to increase as the test advances. This fact may be indicative of hydrogen stratification in the line since the points where the samples are taken are located at the top of the pipes. More data are, however, necessary to reach a conclusion.



Figure 25. Picture of part of the static section of the testing platform. Red arrows show the point where hydrogen leakages were detected

The complete test will be included in D4.4, where the results will be analysed in depth and proper conclusion will be stated.

Pending

5 Slow Strain Rate Tests

As a complement to the constant displacement test specimens used for the evaluation of hydrogen embrittlement sensibility, a rising load test method such as the Slow Strain Rate Test (SSRT) is proposed for the API 5L steels. The SSRT is a particularly important screening method to measure susceptibility to hydrogen embrittlement. Specimens are tensile strained to failure with “slow” strain rates, commonly in the range 10^{-6} - 10^{-4} s⁻¹. The results of the SSRT are evaluated comparing the results obtained in an inert environment (air/N₂) and in hydrogen gas. The reduction of area ratio (RRA) and the notched tensile strength ratio (NTS), are used as a measure of hydrogen susceptibility in smooth or notched specimens, respectively.

In the case of the API 5L steels under study, notched tensile specimens will be used to localize the failure in the base or weld zones. Tests will be carried out in 100% H₂, at a test pressure of 80 bar and using a strain rate of 10^{-6} s⁻¹, following ASTM G142 and ASTM G129 standards.

These tests are expected to start in month 46 and continue until month 47. The results will be included in D4.4.

Pending for approval

6 Conclusions

The tolerance towards hydrogen of the API 5L steels grades X42, X52, X60 and X70, valves and equipment installed in the HIGGS' R&D platform built at FHA, has been evaluated for the operating conditions established in the 2nd and 3rd experimental campaigns. The 2nd experimental campaign consisted in the 20/76 (mol%/%) H₂/CH₄ blend gas condition, with H₂S up to 11 ppmv and CO₂ (4 mol%) impurities. The gas mixture for the 3rd campaign was made up of 30/66 (mol%/%) H₂/CH₄, with the same concentration of impurities than those contemplated for the 2nd campaign. Test pressure for both experimental campaigns was 80 bar.

The visual inspection of the pilot-operated pressure regulator and cartridge filter components from the dynamic section tested during the 2nd campaign, indicates that there is no apparent damage on the different parts examined.

With regard to the ball valve which presented the gas leakage at the end of the 2nd campaign, the dismantling of the valve showed a non-uniform deformation in the Teflon seat located near the closure, probably due to a misalignment between the ball and the seat. Therefore, the failure could not be attributed to a hydrogen damage.

Regarding the steels, the constant displacement C-Ring and 4pb specimens showed no effect of cracking or embrittlement after visual inspection and metallographic cross-section examination, neither in the base material, the HAZ, nor the welded material. No crack propagation could be noticed in CT-WOL specimens either, being the extension of the crack below the limits of acceptance of the standard. It can be therefore concluded that in the tests to evaluate the compatibility of the steels using constant deformation specimens, no signs of embrittlement are observed after 2nd and 3rd experimental campaigns.

Most valves and couplings seem tight to hydrogen during this first stage of the 3rd campaign, except for the screwed ball valves that a showing a clear lack of internal tightness. Besides, hydrogen stratification might be happening, although additional data are necessary to identify this problem.

Bibliography and References

- API 5L, Specification for line pipe (2020)
- ISO 7539-2, Corrosion of metals and alloys. Stress corrosion testing. Part 2: Preparation and use of bent-beam specimens (1996)
- ISO 7539-5, Corrosion of metals and alloys. Stress corrosion testing. Part 5: Preparation and use of C-ring specimens (1996)
- ISO 7539-6, Corrosion of metals and alloys. Stress corrosion testing. Part 6: Preparation and use of precracked specimens for tests under constant load or constant displacement (2020)
- ASTM G38, Standard practice for making and using C-Ring stress-corrosion test specimens. (2021)
- ASTM G39, Standard practice for preparation and use of bent-beam stress-corrosion test specimens (2021)
- ASTM E1681, Standard test method for determining threshold stress intensity factor for environment assisted cracking of metallic materials (2020)
- ASTM E399, Standard test method for linear-elastic plane-strain fracture toughness of metallic materials (2022)
- ASTM G142, Standard test method for determination of susceptibility of metals to embrittlement in hydrogen containing environments at high pressure, high temperature, or both (2022)
- ASTM G129, Standard practice for Slow Strain Rate Testing to evaluate the susceptibility of metallic materials to environmentally assisted cracking (2021)

Acknowledgements

This project has received funding from the Fuel Cells and Hydrogen 2 Joint Undertaking (now Clean Hydrogen Partnership) under Grant Agreement No. 875091 'HIGGS'. This Joint Undertaking receives support from the European Union's Horizon 2020 Research and Innovation program, Hydrogen Europe and Hydrogen Europe Research.



Pending for approval